FAST TRANSVERSE INSTABILITY AND ELECTRON CLOUD MEASUREMENTS IN FERMILAB RECYCLER

J. Eldred, Department of Physics, Indiana University, Bloomington, IN 47405, USA
P. Adamson, D. Capista, N. Eddy, I. Kourbanis, D.K. Morris, J. Thangaraj, M.J. Yang, R. Zwaska, FNAL, Batavia, IL 60510, USA
Y. Ji, Department of Physics, Illinois Institute of Technology, Chicago, IL 60616, USA

Abstract

A new transverse instability is observed that may limit the proton intensity in the Fermilab Recycler. The instability is fast, leading to a beam-abort loss within two hundred turns. The instability primarily affects the first high-intensity batch from the Fermilab Booster in each Recycler cycle. This paper analyzes the dynamical features of the destabilized beam. The instability excites a horizontal betatron oscillation which couples into the vertical motion and also causes transverse emittance growth. This paper describes the feasibility of electron cloud as the mechanism for this instability and presents the first measurements of the electron cloud in the Fermilab Recycler. Direct measurements of the electron cloud are made using a retarding field analyzer (RFA) newly installed in the Fermilab Recycler. Indirect measurements of the electron cloud are made by propagating a microwave carrier signal through the beampipe and analyzing the phase modulation of the signal. The maximum betatron amplitude growth and the maximum electron cloud signal occur during minimums of the bunch length oscillation.

INTRODUCTION

Beginning in July 2014, a fast intensity-induced transverse instability was observed in the proton beam of the Fermilab Recycler. This instability is currently a limiting factor on the stable proton intensity in the Recycler. The Recycler is currently being commissioned from slip-stacking [1, 2]. The instability has the unusual feature of selectively impacting the first high-intensity batch. Our studies focus on electron cloud because it is the most probable mechanism for the Reycler instability.

A qualitatively similar phenonenon, refered to as a "first pulse" electron cloud instability, has been observed at Los Alamos National Laboratory (LANL) [3, 4]. It should be noted, however, that the LANL macropulse timing structure is a very different timescale from the Fermilab batch timing structure [5].

The azimuthal space in the Fermilab Booster is divided into 84 buckets with typically 82 of those buckets are filled during operation. The Booster extracts to the Recycler (or the Main Injector) at a rate of 15 Hz and each Booster pulse is known as a batch. Six 84-bucket Booster batches and a 84-bucket kicker gap fill the 588-bucket azimuthal space of the Booster Recycler. During slip-stacking operation another six Booster batches can be injected.

When the first batch exceeds a certain intensity threshold (originally 3e12), the Recycler instability causes the horizontal betatron dipole oscillation to grow dramatically and can lead to ~ 25% loss within the first 150 turns. At this point, the beam is aborted to minimize loss activation as described in [1]. The rapid amplitude growth of the instability is only consistent with electron cloud [6, 7, 8]. Below the intensity threshold, the increased betatron oscillation amplitude is only apparent in the first batch.

If the first batch is just below threshold, the subsequent batches can have intensities above the single-batch intensity threshold without significant beam loss. When the Recycler beam is running in this configuration the most significant betatron excitation appears in the second batch, followed by the first batch. This configuration, with the first batch at ~ 80% intensity of subsequent batches, enables the greatest total beam intensity at normal loss rates. On July 24th the Recycler titanium sublimation pumps were fired [9] and on August 1st the Recycler switched to running with the first batch at lower intensity then subsequent batches. The maximum beam intensity was 22e12 protons on August 1st 2014 but gradually increased to 26e12 protons by August 10th 2014. The change in the instability threshold is consistent with beampipe conditioning effects which increase the threshold associated with electron cloud [10, 11].

The Recycler is outfitted with a digital damper system designed to mitigate transverse instabilities during antiproton accumulation (see [12]). The damper system is at least an order of magnitude too weak to prevent losses from this new instability in the Recycler. This Recycler instability also occurs when the damper system is turned off.

The shorter bunch lengths appear to lower the intensity threshold of the Recycler instability. In one illuminating study (July 16th 2014), six batches each with 3.3e12 protons were injected into the Recycler with a deliberate RF phase mismatch to induce a bunch length oscillation. Figure 1 shows that the instability immediately overpowers the damper when the bunch length is short but the betatron motion damps and decoheres when the bunch length is long. This figure also demonstrates that the instability begins in the horizontal plane but the betatron motion spreads to the vertical plane via the linear coupling of the lattice [13]. It appears in this case that the instability begins the middle of the batch and migrates to the tail of the batch. If the instability has increased the emittance in the center of the batch than this would delay the onset of the electron cloud and could account for the movement of the instability towards the tail of the batch.

ISBN 978-3-95450-173-1

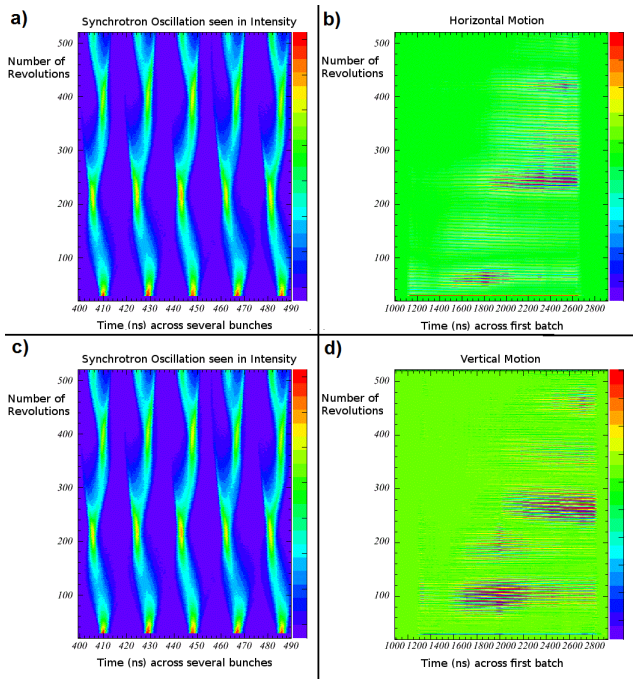

Figure 1: Plots produced from resistive wall current monitor and stripline BPM signals used in the digital damper system.**a,c)** Intensity plot as a function of revolution number and time within each revolution. **b)** Horizontal motion as a function of revolution number and time within each revolution. **d)** Vertical motion as a function of revolution number and time within each revolution.

The Recycler instability is encountered in the Recycler during normal tuning conditions. For the measurements described in this paper, the horizontal and vertical chromaticities are approximately -5. Further description of the Recycler lattice and tuning parameters can be found in [14]. The vacuum in the Recycler was measured to be good quality, typically 1e-10 torr at the ion pumps.

In the next section we describe the symptoms of the instability measured by beam position instrumentation. In particular we map out changes in the betatron oscillation amplitude, the particle losses, and the bunch length. In following two sections we present two methods measuring electron cloud in the Recycler. In the first method the electron cloud is detected directly by a retarding field analyzer (RFA) and in the second method the presence of the electron cloud is infered by the phase-modulation of a microwave signal traveling through the beampipe. Penultimately, we present simulation results describing a plausible mechanism by which electron cloud could exhibit the batch-selective feature observed in the Recycler instability. In the final section, we summarize and describe future actions.

STRIPLINE MEASUREMENTS OF BEAM POSITION

An in-depth study of the Recycler instability was conducted on July 18th 2014 by studing the motion of the beam with a stripline beam position monitor. The specifications and calibration procedures of the stripline BPM are described in [15].

In this study, a single batch was injected with an intensity of 3.2e12 which is just above the theshold intensity (at the time). The digital damper system was turned off and beam loss abort occurs after 165 revolutions. The bunches undergo a bunch-length oscillation due to the mismatch between the Recycler and the Booster. In this study the vertical motion was small compared to the horizontal motion. The motion within the bunch was relatively uniform - the amplitude and tune of the oscillation was consistent head to tail.

Figure 2. shows the horizontal position averaged within each bunch and displayed across one batch. Oscillations are too fine to make out by eye. Figure 3 shows average Fourier transform of the horizontal position. The Fourier spectrum reveals the horizontal motion is dominated by low frequency components and oscillations at the betatron tune.

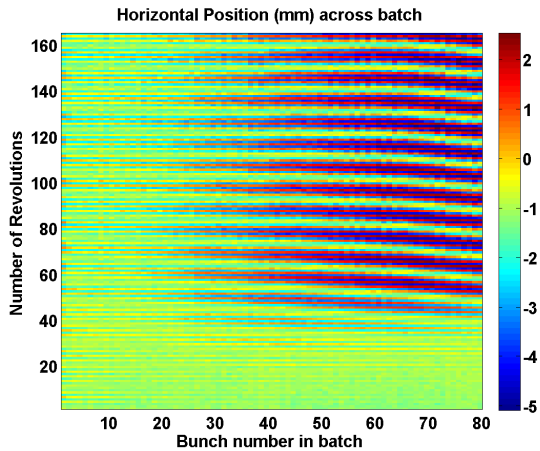

Figure 2: Stripline measurements of horizontal beam position visualized across the batch and across times.

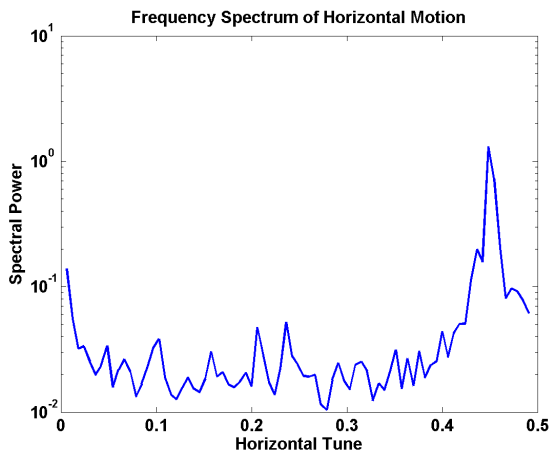

Figure 3: For several points of each bunch, the horizontal frequency spectrum is taken and summed. The peak shown in this plot is located at 0.4485 which corresponds to the horizontal betatron tune.

ISBN 978-3-95450-173-1

The instability manifests as a growing betatron dipole oscillation and therefore the amplitude and tune of the betatron oscillation can be used as an effective metric of the instability. We divide the dataset into overlapping 12-revolution windows and for each window we calculate the best-fit betatron tune and its amplitude.

Figure 4 shows the horizontal betatron amplitude across the batch. The betatron amplitude grows rapidly (~ 20 revolution doubling time) and appears to level off around the 70th revolution. The betatron amplitude growth is concentrated in the second half of the batch and obtains the maximum betatron oscillation amplitude between the 60th and 70th bunch in the batch. The moiré patten in Figure 4 is most likely an aliasing effect.

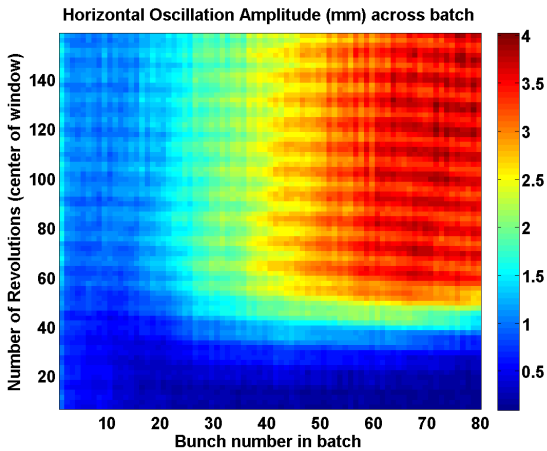

Figure 4: Horizontal betatron amplitude across batch and over time.

Figure 5 shows the particle losses across the batch. The particle losses are calculated by changes in the stripline sum signal. The losses occur in the second half of the batch and increase as the betatron amplitude growth rate decreases. Figure 6 shows the batch-average of the betatron amplitude growth rate juxtaposed with the batch-total of the particle loss. The decrease in the betatron amplitude growth rate is not consistent with a selection effect from the loss of particles with high betatron amplitudes.

Figure 7 shows the bunch length across the batch. The bunch length is calculated as the standard deviation of the (stripline) intensity distribution. The bunch lengths are consistent across the batch but vary from ~ 1.4 ns to ~ 1.9 ns over a half synchrotron period. Figure 8 show the batch-average of the betatron amplitude growth rate juxtaposed with the batch-average of the bunch length. The minimum of the bunch length oscillation coincides with the maximum betatron amplitude growth rate.

The Recycler instability can be compared to the electron cloud instability seen in the CERN SPS by Cornelis [7]. Our results seem consistent with the horizontal motion but not the vertical motion. Simulations of electron cloud instabilities also predict rapid transverse emittance growth [8, 16, 17].

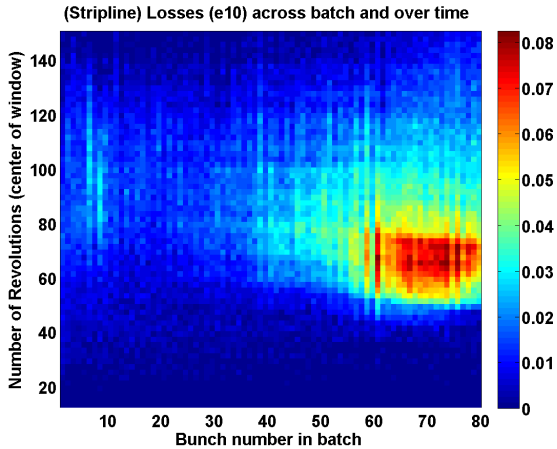

Figure 5: Particle losses across batch and over time.

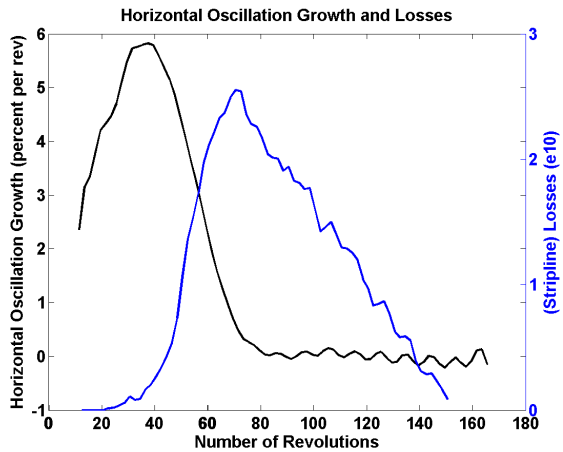

Figure 6: The left axis (black) indicates the betatron amplitude growth rate averaged across the batch and the right axis (blue) indicates the particle losses summed across the batch.

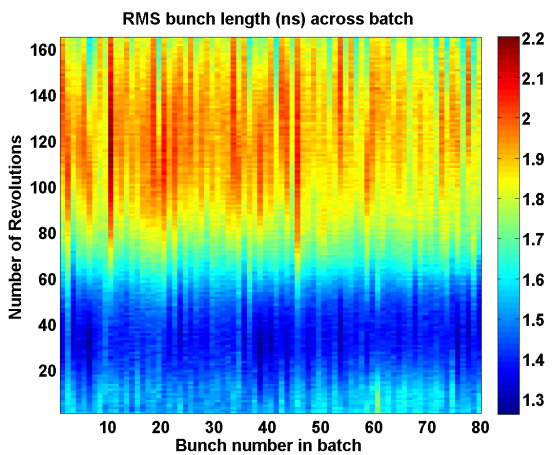

Figure 7: Bunch length across batch and over time.

ISBN 978-3-95450-173-1

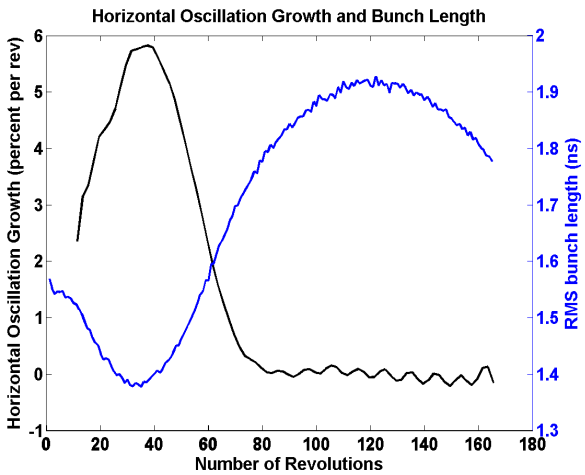

Figure 8: The left axis (black) indicates the betatron amplitude growth rate averaged across the batch and the right axis (blue) indicates the bunch length averaged across the batch.

DIRECT MEASUREMENT OF ELECTRON CLOUD

From September 5th to October 23rd there was a prescheduled shutdown period in which an RFA electron cloud detector was installed in the Recycler at MI-52. Details about the design and characterization of the RFAs are given in [18] and [11]. Other accelerators have deployed similar collectors to study electron cloud [19, 20, 21]. An RFA signa of 1V is estimated to represent an electron flux of $\sim 1e7$ electrons per second per square centimeter. The RFA was installed on 100 ft of new stainless steel beampipe with no previous history of electron cloud conditioning. This RFA has been exposed to less than a week of scrubbing and we have not yet run high-intensity multiple-batch Recycler cycles since the shutdown. Consequently we expect the electron cloud measured by the newly installed RFA would be typical of a higher SEY than would generally be found in the rest of the Recycler.

Figure 9 and Figure 10 show the RFA response to a single 3.1e12 batch cycle and a six batch 2.6e12 cycle respectively. In Figure 9 we see that when the batch is injected the electron cloud RFA is composed of several sharp peaks spaced at half synchrotron period intervals and declining in height. In Figure 10 we see a similar signal at each batch injection but with the signals rising with each subsequent injection.

The sharp peaks in the electron cloud signal occur at minimums of the bunch length oscillation. An increase in electron cloud density is the expected response to a reduction in bunch length [22]. The greatest oscillation amplitude growth due to the Recycler instability also occurs at bunch length minimums (Figure 1 and Figure 8).

In Figure 10, the sharp peaks in electron cloud signal decline in height more gradually than in Figure 9. The gradual decline in the electron cloud peak height may be explained by filamentation of the synchrotron oscillation. The initial, very rapid decline in the electron cloud peak height appears

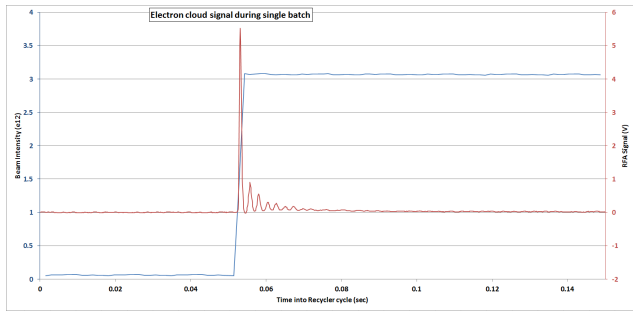

Figure 9: The left axis (blue) indicates the total beam intensity stored in the Recycler and the right axis (red) indicates the magnitude of the RFA ecloud signal. The traces correspond to a single 3.1e12 batch Recycler cycle.

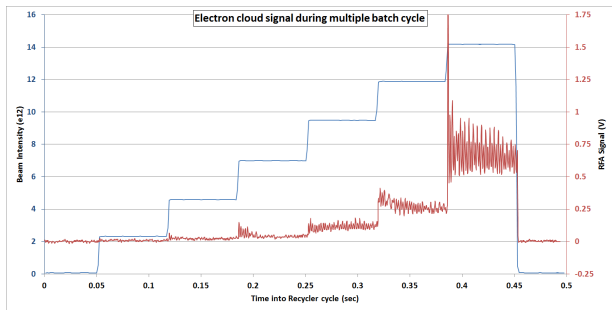

Figure 10: The left axis (blue) indicates the total beam intensity stored in the Recycler and the right axis (red) indicates the magnitude of the RFA ecloud signal. The traces correspond to a six batch 2.6e12 Recycler cycle.

to only occur at high beam intensities. One explanation is that the first electron cloud peak dramatically increases the transverse emittance of the beam. In the next electron cloud peak, the beam has a larger transverse emittance and therefore does not produce an electron cloud of the same density (see [8]). This model of close feedback between the transverse beam emittance and the electron cloud density is a novel regime of electron cloud dynamics.

MICROWAVE MEASUREMENTS OF ELECTRON CLOUD

On August 20th 2014 a study of the Recycler electron cloud was conducted with microwave electronics. At the time of these measurements, the first batch is was operating at an intensity of $\sim 3.6e12$ and subsequent batches at an intensity of $\sim 4.5e12$ per batch. On each day, two "split-plate" BPMs in the Recycler (VP201 and VP203) [23] were disconnected and used to transmit a microwave signal through the beampipe in order to infer the presence of electron cloud in the Recycler. These studies follow the technique implemented in the Fermilab Main Injector by Crisp et. al. in [24] and also by others [25, 26, 27].

Unlike the RFA electron cloud measurement shown in this paper, the microwave technique can measure the electron cloud in dipole regions with typical beampipe conditioning.

ISBN 978-3-95450-173-1

In addition, we currently have only measured high-intensity multiple-batch cycles with the microwave technique.

A schematic of the electronic setup used for these studies is shown in Figure 11. The signal generator is used to drive a ~ 1.9GHz carrier signal which is then passed through an amplifier and a high-pass filter. This carrier signal is sent into a Recycler BPM used as a microwave transmitter, is propagated through the Recycler beampipe, and is received by the second Recycler BPM used as a microwave receiver. This carrier signal then passes through another high-pass filter and is recorded by the signal analyzer. Using the split-plate BPMs as improvised microwave antennas results in a ~ −80 dB transmission loss.

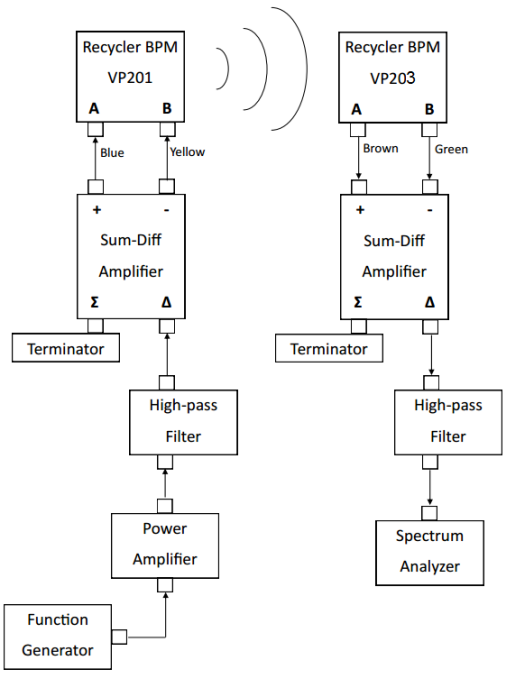

Figure 11: Flow-chart schematics of the microwave electronics used to measured the electron cloud. The signal generator creates a signal at a single carrier frequency, next this signal propagates through the electron cloud, and lastly this signal is examined for phase modulation in the signal analyzer.

In the presence of an electron cloud of uniform density, the carrier signal receieves a phase delay approximately [26] given by

$$\phi \approx \frac{L}{c} \frac{\omega_p^2}{2\sqrt{\omega^2 - \omega_c^2}} \tag{1}$$

where L is the path length and ω_c is the cut-off frequency of the beampipe. The plasma frequency ω_p can be approximated (in Hz) by

$$\omega_p \approx 2\pi 9 \sqrt{\rho_e} \tag{2}$$

where ρ_e is the density of the electron cloud in electrons per cubic meter.

The density of the electron cloud is modulated by the revolution harmonics of the proton beam (~90 KHz) and therefore the carrier frequency is phase-modulated (PM) in the presence of the electron cloud. Consequently, the electron cloud signal is seen as 90kHz sidebands on either side of the carrier frequency. The contribution that each batch makes to the sideband is $2\pi/7$ out of phase with the contribution made by the adjacent batch. This creates a possible ambiguity betweeen changes in the density of the electron cloud and change in the distribution of the electron cloud.

From Eq. 1 it can be seen that the optimal carrier signal is near the cut-off frequency of the beampipe because that greatly enhances the magnitude of the electron cloud phase-delay while keeping the amplitude of the carrier signal high. For the measurements presented in this paper we used 1.977 GHz as our carrier frequency, but our choice of carrier frequency may not be completely optimized.

For a 1.977000 GHz carrier frequency and a 90 kHz modulation frequency, the lower sideband frequency is 1.976910 GHz. Figure 12 shows the average spectral power of the lower sideband frequency as a function of time within the Recycler cycle. The beam background trace may be indicating the operation of the Recycler kickers because the sharp peaks coincide with the six batch injections into the Recycler as well as the batch extraction from the Recycler. The electron cloud measurement trace also shows sharp peaks at batch injection and these peaks are a statistically significant margin above the sharp peaks in the beam background trace.

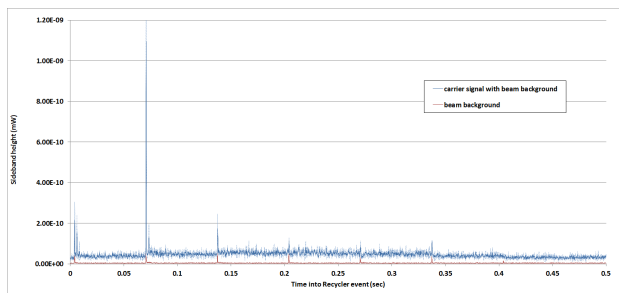

Figure 12: Spectral power of the lower sideband frequency averaged over 40 Recycler cycles and for each of two conditions. In the "beam background" condition (red), the spectal power is measuring cycle-dependent background from the beam harmonics and accelerator electronics. In the "carrier signal with beam background" a carrier signal is also propagated through the beampipe and the trace includes the sideband of this signal.

Figure 13 zooms in on the gradual features of the traces shown in Figure 12 to reveal "plateaus". The plateaus are the piecewise constant features that increase in magnitude up to third and fourth batch and then decrease in subsequent batches. Recall that the contribution of each batch to the sideband height is $2\pi/7$ out of phase with the previous batch. Consequently, these plateaus are actually consistent with the case in which each batch generates a comparable amount of

ISBN 978-3-95450-173-1

electron cloud while passing a given section of beampipe. In that case, the plateaus are indicating an electron cloud density relatively uniform across the second and subsequent batches (with electron cloud flux increasing proportionally with the number of batches) [28].

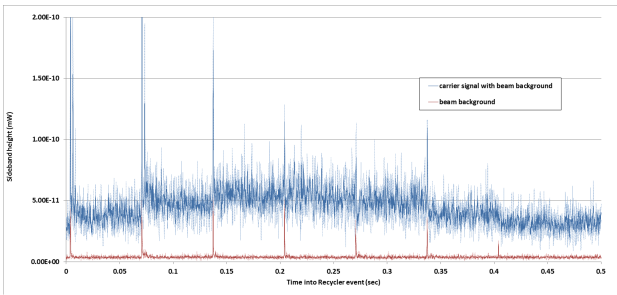

Figure 13: Spectral power of the lower sideband frequency averaged over 40 Recycler cycles with and without a carrier signal. This plot zooms in on the plateaus of the measurement trace.

Figure 14 zooms in the sharp peaks at the first two batch injections shown in Figure 12 and Figure 13. At each injection, there are actually two or three sharp peaks each declining in height with respect to the previous peak. The peaks are spaced at half-synchrotron period intervals because they coincide with the minimums of the bunch length oscillation.

The sharp peaks of the measurement trace (Figure 12) that occur at the second injection are always significantly higher than that of the first injection; the peaks at the first injection are higher still than those at the third and subsequent injections. The profile of injection peak heights matches the profile of the instability observed in the beam while these measurements were taken. These measurements are taken with the first batch at $\sim$ 80% the intensity of subsequent batches, with the largest betatron oscillation amplitude observed in the second batch.

However, it is difficult to identify a mechanism which would account for this selective generation of electron cloud. Moreover, this profile of the electron cloud does not match the profile observed in the low-intensity multiple-batch RFA signal (Figure 10). If the electron cloud density after the first two batches is sufficiently great, its possible that the electron cloud instability could rapidly increase the emittance of the third batch in the $\sim$ 30 revolutions before its first bunch length minimum. However, one would naively expect that this rapid emittance growth would co-occur with rapid betatron amplitude growth which is not observed in the third batch. Another hypothesis would be that the electron cloud temporarily modifies the SEY of the beampipe by desorbing large quantities of gas. However the maximum electron cloud density would be many orders of magnitudes too small to alter the SEY of the beampipe on this timescale.

During the shutdown, spare split-plate BPMs in the Recycler (VP130 and VP202) were connected to the microwave electronics (Figure 11). Consequently, future microwave measurements of electron cloud in the Recycler will not require disconnecting any instruments currently used to monitor beam position.

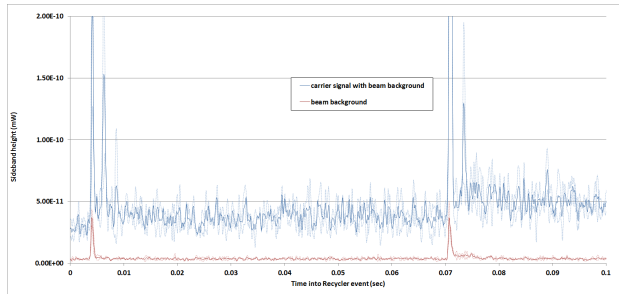

Figure 14: Spectral power of the lower sideband frequency averaged over 40 Recycler cycles with and without a carrier signal. This plot zooms in on the features of the sharp peaks at batch injection.

Table 1: Recycler and Parameters Used for POSINST Simulation of Electron Cloud Striping

Beam Kinetic Energy (E)	8 GeV
Beam Distribution Transverse sigma (σ_x)	3 mm
Beam Distribution Longitudinal sigma (σ_z)	0.75 m
Full Bunch Intensity	5e10
Buckets per batch	84
Filled buckets per batch	82
Number of batches	6
Beampipe SEY (maximum)	2.2
Beampipe geometry	elliptical
Beampipe horizontal major axis	94 mm
Beampipe vertical major axis	44 mm
Dipole field strength	1.375 T

SIMULATION DATA OF ELECTRON CLOUD STRIPING

In this section we present one mechanism for the electron cloud instability to be batch-selective. Electron cloud has been observed forming stripes in the presence of a strong dipole field [19]. Simulations indicate that in low electron cloud densities, the electron cloud is confined to a single vertical stripe centered on the beam. As the electron cloud density starts to near a maximum saturation point, the structure of the electron cloud changes to two vertical stripes with a bimodal horizontal distribution [29].

We conducted electron cloud simulations using POSINST [30], an electron cloud simulation program that relies on the Furman-Pivi model of secondary electron yield (SEY) [31]. The simulations presented in this paper use realistic parameters for the Recycler, shown in Table 1, with the possible exception of the SEY. The SEY for the simulation was 2.2, the SEY of completely unconditioned stainless steel [32]. We find that the electron cloud generated in each revolution is independent of the previous revolution.

ISBN 978-3-95450-173-1

The simulations indicate that the electron cloud density in the beampipe increases every revolution until the end of the last batch, at which point it falls off rapidly. The electron cloud density within in the one sigma ellipse of the beam, however, can obtain an early maximum. Figure 15 shows the electron density within one sigma of the beam for a cycle in which all batches have the same intensity (5e10 per bunch). Figure 16 shows the electron density within one sigma of the beam for a cycle in which the first batch has 75% the intensity of subsequent batches (3.5e10 per bunch). In Figure 15 the peak electron cloud density near the beam is obtained during the first batch and in Figure 16 the peak electron cloud density near the beam is obtained during the second batch. This matches the batch-selectivity observed in the Recycler instability - a modest decrease in the intensity of the first batch moves the instability from the first batch to the second batch and the instability becomes less severe.

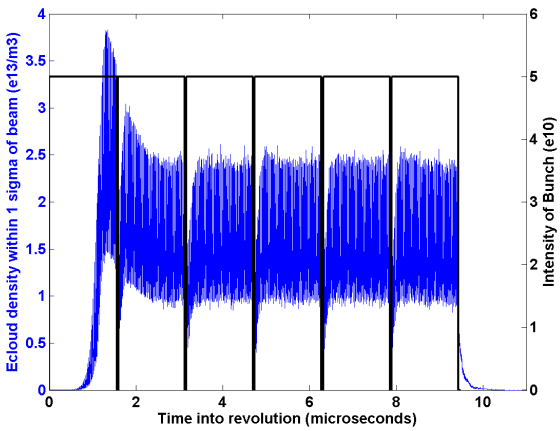

Figure 15: Simulated electron cloud density within 1 sigma of the beam (blue) for a beam structure with six batches of equal intensity (black). The maximum electron cloud density (within 1 sigma of the beam) is 3.83e13 per cubic meter and is obtained after the 71st bunch. The batches are 84 (18.8ns) buckets long with 82 buckets filled with 5e10 intensity bunches.

The electron cloud density within one sigma of the beam peaks because of the formation of stripes in the dipole field. Figure 17 shows simulated particles distributed in a single stripe at the 60th bucker and Figure 18 shows simulated particles distributed in two stripes at the 212th bucket. Both distributions are drawn from the same simulation run shown Figure 16. The discrete lines that compose the stripes in Figure 17 and Figure 18 are not numerically stable features of the simulation and should be regarded as a approximate description of the more continuous distributions shown in [29] and [17]. We have also conducted simulations without a strong dipole field and we do not find particles distributed in stripes or find an early peak in the electron cloud density near the beam.

This dipole-striping model presently represents our best explanation for the observed batch-selectivity of the electron cloud instability [33]. It should be noted that this model predicts only the batch-selectivity of the electron cloud instability (seen in the microwave data).

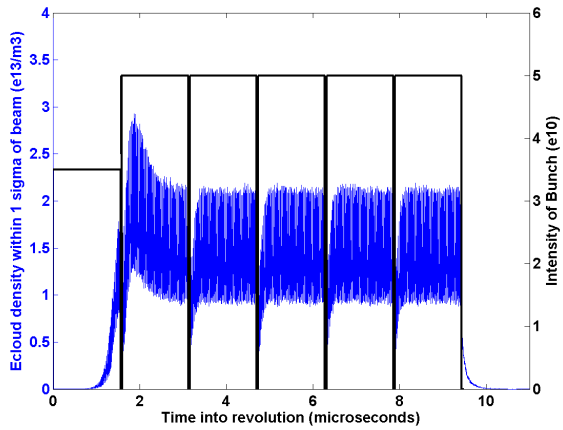

Figure 16: Simulated electron cloud density within 1 sigma of the beam (blue) for a beam structure with the first batch at 75% the intensity of subsequent five batches (black) The maximum electron cloud density (within 1 sigma of the beam) is 2.93e13 per cubic meter and is obtained after the 98th bunch. The batches are 84 (18.8ns) buckets long with 82 buckets filled with 3.5e10 and 5e10 intensity bunches.

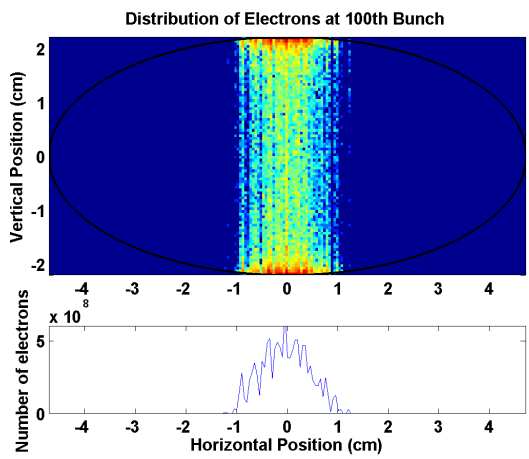

Figure 17: (top) 2D histogram showing the positions of particles in an electron cloud simulated by POSINST. The color indicates the number of particles on a log scale. (bottom) 1D histogram showing the horizontal distribution of particles. The particles are located within a single vertical stripe and have a unimodal horizontal distribution.

CONCLUSIONS

We will continue to study this new instability and the electron cloud in the Recycler. The September-October shutdown provided an opportunity for dedicated RFA and microwave electron cloud instrumentation to be installed in the Recycler. Within a week or two we will be able to observed the RFA signal near the multiple batch intensity threshold.

ISBN 978-3-95450-173-1

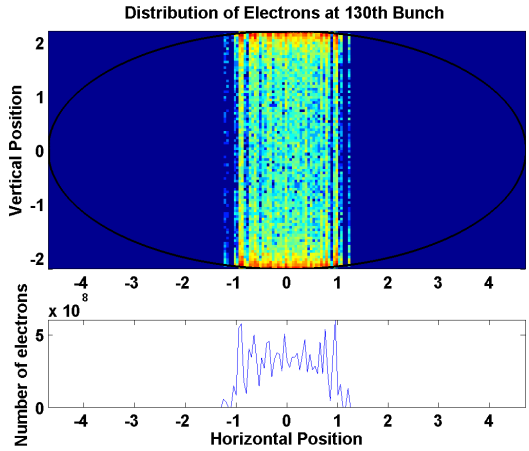

Figure 18: (top) 2D histogram showing the positions of particles in an electron cloud simulated by POSINST. The color indicates the number of particles on a log scale. (bottom) 1D histogram showing the horizontal distribution of particles. The particles are located within two overlapping vertical stripes and have a bimodal horizontal distribution.

If the instability is indeed caused by electron cloud, it is possible that commissioning of the Recycler for slip-stacking in the coming months will sufficiently condition the beampipe to effectively eliminate losses from the instability. If so, this paper has provided the first glimpse into the nature of electron cloud instabilities at Fermilab Recycler. If incidental beampipe conditioning is not sufficient to raise the instability threshold, we are considering dedicated scrubbing cycles with the purpose of advancing the rate of conditioning. We have also discussed the possibility of upgrading the digital damper system in the Recycler.

This paper has informed the greater accelerator community of a new instability both worth avoiding and worth studying. We describe the salient dynamical features of the instability in detail. The connection between the electron cloud in the Recycler is compelling. The electron cloud in the Recycler shows a dramatic dependence on bunch length and transverse emittance. This works underscores the need to understand the diversity of electron cloud phenomena.

REFERENCES

[1] B. C. Brown, P. Adamson, D. Capista et al., Phys. Rev. ST Accel. Beams **16**, 071001 (2013) http://journals.aps.org/prstab/abstract/10.1103/PhysRevSTAB.16.071001

[2] J. Eldred, R. Zwaska, these proceedings, MOPAB12, Proc. HB14.

[3] R. J. Macek, A. A. Browman, M. J. Borden et al., Proc. ECLOUD04, http://mafurman.lbl.gov/ECLOUD04_proceedings/Macek_StatusReport-PSR-v3.pdf

[4] R. J. Macek, T. Spickermann, A. Browman et al. Proc. HB2006, www.jacow.org/abdwhb06/PAPERS/THAW04.PDF

[5] R. McCrady, B. Blind, J. D. Gilpatrick et al., Proc. BIW10, http://www.jacow.org/BIW2010/papers/weianb01.pdf

[6] R. McCrady, R. Macek, T. Zaugg et al., Proc. PAC07, http://www.jacow.org/p07/PAPERS/MOPAS050.PDF

[7] K. Cornelis, Proc. ECLOUD2, http://conf-ecloud02.web.cern.ch/conf-ecloud02/papers/allpdf/cornelis.pdf

[8] G. Rumolo, G. Arduini, E. Métral et al., Phys. Rev. Lett. **100**, 144801 (2008) http://journals.aps.org/prl/pdf/10.1103/PhysRevLett.100.144801

[9] G. Jackson, Fermilab Recycler Ring Technical Design Report, Fermi National Accelerator Facility, 1996 http://inspirehep.net/record/428434

[10] R. Zwaska, Proc. PAC11, http://www.jacow.org/PAC2011/papers/moobs4.pdf

[11] M. Backfish, Masters thesis, Indiana University, 2013 http://inspirehep.net/record/1294079/files/fermilab-masters-2013-03.pdf

[12] P. Adamson, W. J. Ashmanskas, G. W. Foster et al., Proc. PAC05, www.jacow.org/p05/PAPERS/MPPP015.PDF

[13] M. Xiao, M. Yang, D. E. Johnson et al., Proc. PAC05, www.jacow.org/p05/PAPERS/MPPE052.PDF

[14] M. Xiao, Proc. IPAC12, http://www.jacow.org/IPAC2012/papers/tuppr085.pdf

[15] J. Crisp, K. Gubrienko, V. Seleznev, Fermilab Report No. BEAMS-DOC-339-v2, 1998, https://beamdocs.fnal.gov/AD-private/DocDB/ShowDocument?docid=339

[16] K. Li, G. Rumolo, Proc. IPAC11, www.jacow.org/IPAC2011/papers/MOPS069.PDF

[17] E. Benedetteo, Ph.D. thesis, Turin Polytechnic, 2006 http://inspirehep.net/record/887199

[18] C. Y. Tan, K. L. Duel, R. Zwaska, Proc. PAC09, www.jacow.org/pac2009/papers/th5rfp041.pdf

[19] J. R. Calvey, W. Hartung, Y. Li et al., arXiv:1408.5741 (2014) https://inspirehep.net/record/1312222

[20] C. Yin Vallgren, G. Arduini, J. Bauche et al. Phys. Rev. ST Accel. Beams **14**, 071001 (2011) http://journals.aps.org/prstab/abstract/10.1103/PhysRevSTAB.14.071001

[21] A. Pertica, S. J. Payne, Proc. ECLOUD12, http://inspirehep.net/record/1254612

[22] F. Caspers, S. Gilardoni, E. Mahner et al., Proc. IPAC12, www.jacow.org/IPAC2012/papers/WEPPR010.PDF

[23] J. Fitzgerald, J. Crisp, E. McCrory et al., AIP Conf. Proc. **451**, 370 (1998) http://scitation.aip.org/content/aip/proceeding/aipcp/10.1063/1.57018

[24] J. Crisp, N. Eddy, I. Kourbanis et al., Proc. PAC09, www.jacow.org/d09/papers/tupb23.pdf

[25] S. De Santis, J. M. Byrd, F. Caspers et al., Phys. Rev. Lett. **100**, 094801 (2008) http://journals.aps.org/prl/pdf/10.1103/PhysRevLett.100.094801

[26] S. Federmann, F. Caspers, E. Mahner, Phys. Rev. ST Accel. Beams **14**, 012802 (2011) http://journals.aps.org/prstab/pdf/10.1103/PhysRevSTAB.14.012802

ISBN 978-3-95450-173-1

[27] S. De Santis, J. Sikora, D. Alesini et al., Proc. IPAC12, www.jacow.org/IPAC2012/papers/MOPPR073.PDF

[28] The plateaus are also consistent with amplitude modulation caused by electronic mixing between the higher beam harmonics and the carrier frequency. However, this interpretation does not seem likely because the RFA data indicates plateaus of genuine electron cloud signal.

[29] P. Lebrun, P. Spentzouris, J. Cary et al. Proc. ECLOUD10, http://www.lepp.cornell.edu/Events/ECLOUD10/proceedings/papers/MOD03.pdf

[30] M. T. F. Pivi, M. A. Furma,S. Federmann, F. Caspers, and E. Mahner https://journals.aps.org/prstab/pdf/10.1103/PhysRevSTAB.6.034201

[31] M. A. Furman, M. T. F. Pivi, Phys. Rev. ST Accel. Beams **5**, 124404 (2002) https://journals.aps.org/prstab/pdf/10.1103/PhysRevSTAB.5.124404

[32] D. J. Scott, D. Capista, K. L. Duel et al., Proc. IPAC12, www.jacow.org/IPAC2012/papers/MOPPC019.PDF

[33] For now we equate increasing electron cloud density near the beam with an increasing severity of the electron cloud instability. But as Burov argues in [34], electron cloud density may not always be a good proxy for the magnitude of the electron cloud instability and instead the presence of the electron cloud may even be stabilizing. Electron clouds introduce both impedance and nonlinearity and these need to be incorporated into a full model of transverse collective instabilities to make an absolute statement about the influence of electron cloud on transverse stability.

[34] A. Burov, Fermi National Accelerator Laboratory Report No. FERMILAB-PUB-13-005-ADD, 2013, http://inspirehep.net/record/1210188/files/fermilab-pub-13-005-ad.pdf

ISBN 978-3-95450-173-1